HHS Public Access

Author manuscript

J Immunol. Author manuscript; available in PMC 2014 May 15.

Published in final edited form as:

J Immunol. 2013 November 15; 191(10): 4913–4917. doi:10.4049/jimmunol.1301927.

Cutting Edge: Type 1 Diabetes Occurs despite Robust Anergy among Endogenous Insulin-Specific CD4 T Cells in NOD Mice

Kristen E. Pauken[*,†], **Jonathan L. Linehan**[*,‡], **Justin A. Spanier**[*,†], **Nathanael L. Sahli**[*,†], **Lokesh A. Kalekar**[*,†], **Bryce A. Binstadt**[*,§], **James J. Moon**[¶], **Daniel L. Mueller**[*,†], **Marc K. Jenkins**[*,‡], and **Brian T. Fife**[*,†]

[*]Center for Immunology, University of Minnesota, Minneapolis, MN 55455

[†]Department of Medicine, University of Minnesota, Minneapolis, MN 55455

[‡]Department of Microbiology, University of Minnesota, Minneapolis, MN 55455

[§]Department of Pediatrics, University of Minnesota, Minneapolis, MN 55455

[¶]Center for Immunology and Inflammatory Diseases, Massachusetts General Hospital and Harvard University, Boston, MA 02114

Abstract

Insulin-specific $CD4^+$ T cells are required for type 1 diabetes. How these cells are regulated and how tolerance breaks down are poorly understood because of a lack of reagents. Therefore, we used an enrichment method and tetramer reagents to track insulin-specific $CD4^+$ T cells in diabetes-susceptible NOD and resistant B6 mice expressing I-A^{g7}. Insulin-specific cells were detected in both strains, but they only became activated, produced IFN-g, and infiltrated the pancreas in NOD mice. Unexpectedly, the majority of Ag-experienced cells in NOD mice displayed an anergic phenotype, but this population decreased with age as tolerance was lost. B6 mice expressing I-A^{g7} were protected because insulin-specific cells did not become effector or anergic T cells but remained naive. These data suggest that NOD mice promote tolerance through anergy induction, but a small proportion of autoreactive T cells escape anergy to provoke type 1 diabetes.

Insulin is an immunodominant Ag during type 1 diabetes (T1D) (1-4). In NOD mice, >90% of insulin-specific $CD4^+$ T cells in the pancreas are specific for the insulin B chain (InsB) peptide 9–23 ($InsB_{9–23}$) (3), and these cells are required for T1D (5). In addition, tolerogenic immunization with $InsB_{9–23}$ peptide delays or prevents T1D (6, 7). Despite the well-established role of insulin-specific $CD4^+$ T cells during T1D, little is known about how this immune response develops because these cells have been difficult to track. There has not been an in-depth analysis of this critical $CD4^+$ T cell population to understand how peripheral tolerance fails and T1D develops.

Address correspondence and reprint requests to Dr. Brian T. Fife, University of Minnesota, 2101 6th Street SE, 3-144 MBB, Campus Code 2641, Minneapolis, MN 55455. bfife@umn.edu.

Disclosures

The authors have no financial conflicts of interest.

MHC class II tetramers are powerful reagents to track Agspecific $CD4^+$ T cells. When coupled with magnetic enrichment, rare cells can be tracked with high precision (8, 9). However, a major challenge in generating MHC class II tetramers is determining the peptide-binding register. The relevant binding register for the $InsB_{9–23}$ epitope is debated (10-13). However, there is evidence that the majority of $InsB_{10–23}$-reactive $CD4^+$ T cells recognize the 14–22 core segment ALYLVCGER (register 3) when mutated to optimize binding to I-A^{g7} (11, 12). Therefore, we constructed a tetramer re-agent containing the modified register 3 epitope bound to I-A^{g7} to define the dynamics of the insulin-specific $CD4^+$ T cell response in diabetes-susceptible NOD mice, as well as resistant B6 mice expressing the I-A^{g7} allele (B6.g7) (14). Our results led to the surprising conclusion that most $InsB_{10–23r3}$: I-A^{g7}–specific T cells are anergic in NOD mice but are naive in B6.g7 mice.

Materials and Methods

Mice

NOD mice were purchased from Taconic. B6.g7 mice were generated by Zucchelli et al. (14). NOD.BDC2.5 mice were purchased from The Jackson Laboratory. NOD.BDC2.5 cells were isolated, as described (15), and 7500 naive T cells were transferred i.v. to 7–12-wk-old prediabetic NOD mice. Blood glucose ≥ 250 mg/dl indicated diabetes (LifeScan). All animal experiments were approved by the Institutional Animal Care and Use Committee of the University of Minnesota.

Insulin tetramer

The $InsB_{10–23r3}$:I-A^{g7} tetramer was constructed similarly as described (8). Briefly, I-A^{g7} monomer containing the peptide HLVERLYLVCGEEG was produced and biotinylated in *Drosophila* S2 cells. Biotinylated monomer was purified on a monomeric avidin column (Thermo Scientific) and combined with streptavidin (SA)-PE and SA-allophycocyanin (Prozyme) to produce the tetramers. The National Institutes of Health tetramer core provided I-A^{g7} henegg lysozyme $(HEL)_{11–25}$ tetramer (AMKRHGLDNYRGYSL).

Flow cytometry

Single-cell suspensions were generated, as described (15). Tetramer-binding cells were enriched from the spleen and nondraining lymph nodes (nondLNs; periaortic, inguinal, brachial, cervical, axillary, and mesenteric lymph nodes) by incubation with 10 nM PE- or allophycocyanin-tetramer for 1 h at 25°C, followed by anti-PE and anti-allophycocyanin MicroBeads for 30 min at 4°C and prior to elution over magnetic columns (Miltenyi Biotec).

Samples were collected using a BD LSR II and Fortessa (BD Biosciences). Data were analyzed using FlowJo software (TreeStar). Cells were enumerated using AccuCheck Counting Beads (Life Technologies).

Cytokine stimulation and priming

Cytokines from insulin-specific $CD4^+$ T cells were assessed in vitro in complete DMEM containing 100 ng/ml PMA, 1000 ng/ml ionomycin, and 10 mg/ml brefeldin A (Sigma) for 4

h (15). For BDC2.5 T cells, 500 μg acetylated p31 peptide (YVRPLWVRME) (Genemed Sythesis) was injected i.v. for 4 h. The modified $InsB_{10–23}$ peptide (11) or $HEL_{11–25}$ (Genemed Synthesis) was emulsified in CFA. Mice were immunized s.c. in the flank (100 μg).

Statistics

Unpaired two-tailed Student t tests were performed with a 95% confidence interval using GraphPad Prism 5 software.

Results and Discussion

Development of the $InsB_{10–23r3}$:I-A^{g7} tetramer reagent

We produced an I-A^{g7} tetramer containing a variant of $InsB_{10–23}$ with substitutions ($InsB_{10–23r3}$) to anchor the peptide in register 3, because previous work showed that this tetramer detects the majority of $CD4^+$ T cells specific for the native peptide (11). Cells from NOD mice were enriched with $InsB_{10–23r3}$:I-A^{g7} or $HEL_{11–25}$:I-A^{g7} tetramers (control), as described (8). Small, but mutually exclusive, populations of tetramer-binding cells were detected among preimmune $CD4^+$ T cells (Fig. 1A). As control, mice were primed with $InsB_{10–23r3}$ and $HEL_{11–25}$, and mutually exclusive tetramer populations expanded (Fig. 1A). Insulin-specific cells became activated, expressed CD44 (Fig. 1B, Supplemental Fig. 1C), and expanded (Fig. 1C).

A small degree of nonspecific binding of the $InsB_{10–23r3}$:I-A^{g7} tetramer was detected on $CD8^+$ T cells (Supplemental Fig. 1A). To increase sensitivity, we stained cells from NOD mice simultaneously with $InsB_{10–23r3}$:I-A^{g7} /SA-PE and SA-allophycocyanin tetramers (Supplemental Fig. 1A). All double tetramer–binding cells expressed CD4 but not CD8. This approach was used for the remainder of the study to eliminate background.

Insulin-specific $CD4^+$ T cells only infiltrate the NOD pancreas

We next evaluated the dynamics of the $InsB_{10–23r3}$:I-A^{g7}–specific $CD4^+$ T cells in diabetes-susceptible NOD and resistant B6.g7 mice. Insulin-specific $CD4^+$ T cells were detected in the pancreatic lymph nodes (pLNs), spleen, and non-dLNs of both strains, consistent with work examining BDC2.5 mimotope–specific $CD4^+$ T cells (Fig. 2A, 2B, Supplemental Fig. 1B) (16). The number of insulin-specific $CD4^+$ T cells increased in the secondary lymphoid organs (SLOs) of NOD mice with age, peaking at 14 wk (Fig. 2A, Supplemental Table IA). There were significantly more insulin-reactive cells in the SLOs of NOD mice at all ages examined compared with B6.g7 mice (Fig. 2A, Supplemental Table IA). In B6.g7 mice, there was a slight, but not significant, increase in cell number between weeks 3 and 5 of life (Fig. 2A). The number of insulin-specific $CD4^+$ T cells did not change in B6.g7 mice between weeks 5 and 20 (Fig. 2A, Supplemental Table IA). Importantly, insulin-specific $CD4^+$ T cells infiltrated the pancreas of NOD mice but not B6.g7 mice (Fig. 2B, Supplemental Fig. 1B). These data demonstrate that insulin-specific $CD4^+$ T cells escape central deletion in both NOD and B6.g7 mice but only infiltrate the pancreas in NOD mice.

We next examined the activation of insulin-specific $CD4^+$ T cells by measuring CD44 expression. Work using BDC2.5 mice showed that activation can be impaired in diabetes-resistant hosts (17). We determined that there was a higher frequency (Fig. 2C, 2D) and number (Supplemental Table IB) of $CD44^{high}$ insulin-specific $CD4^+$ T cells in NOD mice than in B6.g7 mice. The frequency of $CD44^{high}$ cells in the pLNs of NOD mice peaked between weeks 3 and 5, resulting in significantly more activated insulin-specific $CD4^+$ T cells in NOD mice than in B6.g7 mice (Fig. 2D). These results suggest that $InsB_{10–23r3}$:$I\text{-}A^{g7}$–specific T cells become activated in the pLNs of NOD mice but not B6.g7 mice.

Insulin-specific $CD4^+$ T cells differentiate into IFN-γ–producing Th1 cells in NOD mice

In NOD mice we observed a subpopulation of insulin-specific $CD4^+$ T cells that became activated and infiltrated the pancreas. We speculated that these activated cells would produce IFN-γ, because this cytokine is involved in T1D pathogenesis (18, 19). Conversely, we predicted that IFN-γ would not be produced by insulin-specific $CD4^+$ T cells in B6.g7 mice because these cells were a naive phenotype (Fig. 2C, 2D). We also examined TNF-α and IL-17A because of their predicted roles for T1D pathogenesis (20, 21). IFN-γ, TNF-α, and IL-17A were all detected in the polyclonal $CD4^+CD44^{high}$ population in both NOD and B6.g7 mice (Supplemental Fig. 1F). Tetramer-binding cells in NOD mice produced IFN-γ and TNF-α but not IL-17A, whereas B6.g7 mice produced little to no IFN-γ or IL-17A (Fig. 3A). IFN-γ was enriched in $CD44^{high}$ cells in NOD mice (Supplemental Fig. 1D). TNF-α production by insulin-specific $CD4^+$ T cells was detected in both strains, suggesting that the cells were viable (Fig. 3A) (22). These data support a model in which insulin-specific $CD4^+$ T cells encounter Ag and differentiate into pathogenic Th1 cells in NOD mice, whereas failure to encounter autoantigen in B6.g7 mice leads to a lack of Th1 differentiation.

Insulin-specific $CD4^+$ T cells can differentiate into $Foxp3^+$ regulatory T cells

Previous reports demonstrated that regulatory T cells (Tregs) influence the development of T1D (20). We examined the possibility that NOD mice had a decreased frequency of insulin-specific Tregs. However, $Foxp3^+$ Tregs developed in both strains, and we did not measure a significant difference between NOD and B6.g7 mice (Fig. 3B). Therefore, we speculate that Ag-specific Tregs alone are not the main mechanism for diabetes resistance in the B6.g7 mouse. In fact, it appears that there are more Tregs in NOD mice compared with B6.g7 mice; however, this difference is not statistically significant.

T cell anergy develops in the pLNs of NOD mice

It is thought that T1D develops as the result of the loss of peripheral tolerance. However, tolerance induction in the endogenous insulin-specific $CD4^+$ T cell population has never been tested. We predicted that the majority of insulin-reactive T cells would escape tolerance and cause diabetes. However, we found that only a small subset of insulin-reactive T cells produced IFN-γ and infiltrated the pancreas (Figs. 2, 3). We speculated that Ag-experienced insulin-specific T cells might become anergized and be retained in the SLOs. To address this possibility, we took advantage of FR4 and CD73, which were recently identified as markers of T cell anergy on $CD4^+CD44^{high}Foxp3^-$ T cells (23). Recent experiments that we performed in healthy hosts also identified $FR4^+CD73^+$ anergic cells within polyclonal $CD4^+$ T cells (L.A. Kalekar, K.E. Pauken, J.L. Linehan, B.T. Fife, M.K.

Jenkins, and D.L. Mueller, unpublished observations). To test this in T1D, we used our recently characterized adoptive-transfer model to study islet-specific $CD4^+$ T cells (15). In this model, a low number of naive T cells from the BDC2.5 mouse were transferred into prediabetic NOD mice to mimic the endogenous population (15). By 3 wk posttransfer, the BDC2.5 $CD4^+$ T cells developed an anergic phenotype ($Foxp3^-FR4^1CD73^1$) (Fig. 4A, 4B). Surprisingly, more BDC2.5 $CD4^+$ T cells in the pLNs were anergic (Fig. 4A, 4B) than were effector phenotype cells ($FR4^-CD73^-CD44^{high}Foxp3^-$). In contrast, anergic phenotype cells were largely absent from the spleen and pancreas (Fig. 4A, 4B). To validate that coexpression of FR4 and CD73 correlated with functional anergy in diabetogenic T cells, we assessed IFN-γ in the pLNs. Following peptide challenge, IFN-γ was not produced by $CD73^+FR4^+$BDC2.5 T cells, suggesting that they were anergic (Fig. 4C, 4D).

We next examined endogenous insulin-specific $CD4^+$ T cells in NOD and B6.g7 mice for the anergic phenotype. Similar to BDC2.5 cells, the majority of insulin-specific cells displayed the anergic phenotype within the pLNs of NOD mice, and these cells were largely absent from the spleen and non-dLNs (Fig. 4E, 4F). It was difficult to assess cytokine production from the insulin-specific population because of low cell numbers; however, anergic polyclonal $CD4^+$ cells were functionally impaired compared with effector cells, similarly to BDC2.5 cells (Supplemental Fig. 1E). We speculate that the small population of effector cells in the pLNs have escaped tolerance and participate in T1D pathogenesis. The frequency of anergic phenotype insulin-specific T cells was significantly higher in the pLNs of young NOD mice (5 wk) compared with older NOD mice (20–26 wk), consistent with the idea that as mice age, more cells break tolerance. These data support a model in which anergy is induced in a large fraction of insulin-specific $CD4^+$ T cells in the pLNs early in life. However, insulin-specific cells can be detected in the pancreas at this age (Fig. 2), demonstrating that tolerance is incomplete, and progression to T1D may require only a small fraction of self-reactive T cells escaping peripheral tolerance. Furthermore, these data suggest that anergy is not sustained as NOD mice age, which may contribute to enhanced infiltration of the pancreas, ultimately causing diabetes.

We next compared the frequency of anergic cells to ascertain whether anergic cells dominated the B6.g7 mice. B6.g7 mice did not have a significant population of anergic insulin-specific cells (Fig. 4F). These data suggest that B6.g7 mice are protected from T1D because insulin-specific cells do not become effector T cells and retain a naive phenotype rather than become anergic cells.

Although the mechanisms that limit autoimmunity in B6.g7 mice but fail in NOD mice remain to be fully elucidated, our data suggest that there is a substantial difference in the presentation of $InsB_{10\text{-}23}$/MHC class II between these mouse strains. Our findings suggest that, in NOD mice, insulin-specific $CD4^+$ T cells encountered Ag in the pLNs between weeks 3 and 5 of life, and a small subset differentiated into $IFNg^+$ effector cells and infiltrated the pancreas, whereas another larger subset became anergic. Despite the induction of anergy in a large fraction of cells in the pLNs, insulin-specific $CD4^+$ T cells in young NOD mice are capable of driving disease. Therefore, we speculate that only a small number of activated effector cells are responsible for T1D in NOD mice. We further speculate that

B6.g7 mice are diabetes resistant because these cells fail to encounter autoantigen and remain naive.

In conclusion, we developed an MHC class II tetramer that allows tracking of $InsB_{10–23r3}$-specific $CD4^+$ T cells. Despite the presence of pathogenic $CD4^+$ T cells in NOD mice, an anergic population emerged specifically in the pLNs. This population diminished over time and was absent from the pancreas. In B6.g7 mice, insulin-specific cells remained naive, suggesting an absence of Ag encounter. Studying how insulin-specific $CD4^+$ T cells become activated in NOD mice, but not in B6.g7 mice, may provide new insight into how tolerance is breached during T1D. It would be interesting to determine whether other $InsB_{9–23}$ registers have the same bias toward anergy induction or whether these cells are more pathogenic (12, 24). Understanding how peptide/MHC binding impacts the effector potential of diabetogenic $CD4^+$ T cells may aid in our therapeutic efforts to restore tolerance in T1D patients.

Supplementary Material

Refer to Web version on PubMed Central for supplementary material.

Acknowledgments

We thank Dr. Vaiva Vezys and Jason Schenkel (Department of Microbiology, University of Minnesota) for critical review of the manuscript and James Heffernan (Department of Medicine, University of Minnesota) for animal care.

This work was supported by the Juvenile Diabetes Research Foundation (22011662 to B.T.F.), the American Diabetes Association (0709JF21 to B.T.F.), the National Institutes of Health (P01 AI35296 to B.T.F., D.L.M., and M.K.J.), and a Stanwood Johnston Fellowship (to K.E.P.)

Abbreviations used in this article

B6.g7 mice	B6 mice expressing the $I\text{-}A^{g7}$ allele
HEL	hen egg lysozyme
InsB	insulin B chain
non-dLN	nondraining lymph node
pLN	pancreatic lymph node
SA	streptavidin
SLO	secondary lymphoid organ
T1D	type 1 diabetes
Treg	regulatory T cell

References

1. Palmer JP, Asplin CM, Clemons P, Lyen K, Tatpati O, Raghu PK, Paquette TL. Insulin antibodies in insulin-dependent diabetics before insulin treatment. Science. 1983; 222:1337–1339. [PubMed: 6362005]

2. Wegmann DR, Norbury-Glaser M, Daniel D. Insulin-specific T cells are a predominant component of islet infiltrates in pre-diabetic NOD mice. Eur. J. Immunol. 1994; 24:1853–1857. [PubMed: 8056042]

3. Daniel D, Gill RG, Schloot N, Wegmann D. Epitope specificity, cytokine production profile and diabetogenic activity of insulin-specific T cell clones isolated from NOD mice. Eur. J. Immunol. 1995; 25:1056–1062. [PubMed: 7537670]

4. Zhang L, Nakayama M, Eisenbarth GS. Insulin as an autoantigen in NOD/human diabetes. Curr. Opin. Immunol. 2008; 20:111–118. [PubMed: 18178393]

5. Nakayama M, Abiru N, Moriyama H, Babaya N, Liu E, Miao D, Yu L, Wegmann DR, Hutton JC, Elliott JF, Eisenbarth GS. Prime role for an insulin epitope in the development of type 1 diabetes in NOD mice. Nature. 2005; 435:220–223. [PubMed: 15889095]

6. Daniel C, Weigmann B, Bronson R, von Boehmer H. Prevention of type 1 diabetes in mice by tolerogenic vaccination with a strong agonist insulin mimetope. J. Exp. Med. 2011; 208:1501–1510. [PubMed: 21690251]

7. Zhang L, Stadinski BD, Michels A, Kappler JW, Eisenbarth GS. Immunization with an insulin peptide-MHC complex to prevent type 1 diabetes of NOD mice. Diabetes Metab. Res. Rev. 2011; 27:784–789. [PubMed: 22069260]

8. Moon JJ, Chu HH, Pepper M, McSorley SJ, Jameson SC, Kedl RM, Jenkins MK. Naive CD4(+) T cell frequency varies for different epitopes and predicts repertoire diversity and response magnitude. Immunity. 2007; 27:203–213. [PubMed: 17707129]

9. Jenkins MK, Moon JJ. The role of naive T cell precursor frequency and recruitment in dictating immune response magnitude. J. Immunol. 2012; 188:4135–4140. [PubMed: 22517866]

10. Levisetti MG, Suri A, Petzold SJ, Unanue ER. The insulin-specific T cells of nonobese diabetic mice recognize a weak MHC-binding segment in more than one form. J. Immunol. 2007; 178:6051–6057. [PubMed: 17475829]

11. Stadinski BD, Zhang L, Crawford F, Marrack P, Eisenbarth GS, Kappler JW. Diabetogenic T cells recognize insulin bound to IAg7 in an unexpected, weakly binding register. Proc. Natl. Acad. Sci. USA. 2010; 107:10978–10983. [PubMed: 20534455]

12. Crawford F, Stadinski B, Jin N, Michels A, Nakayama M, Pratt P, Marrack P, Eisenbarth G, Kappler JW. Specificity and detection of insulin-reactive CD4+ T cells in type 1 diabetes in the nonobese diabetic (NOD) mouse. Proc. Natl. Acad. Sci. USA. 2011; 108:16729–16734. [PubMed: 21949373]

13. Mohan JF, Petzold SJ, Unanue ER. Register shifting of an insulin peptide-MHC complex allows diabetogenic T cells to escape thymic deletion. J. Exp. Med. 2011; 208:2375–2383. [PubMed: 22065673]

14. Zucchelli S, Holler P, Yamagata T, Roy M, Benoist C, Mathis D. Defective central tolerance induction in NOD mice: genomics and genetics. Immunity. 2005; 22:385–396. [PubMed: 15780994]

15. Pauken KE, Jenkins MK, Azuma M, Fife BT. PD-1, but not PDL1, expressed by islet-reactive CD4+ T cells suppresses infiltration of the pancreas during Type 1 Diabetes. Diabetes. 2013; 62:2859–2869. [PubMed: 23545706]

16. Stratmann T, Martin-Orozco N, Mallet-Designe V, Poirot L, McGavern D, Losyev G, Dobbs CM, Oldstone MB, Yoshida K, Kikutani H, et al. Susceptible MHC alleles, not background genes, select an autoimmune T cell reactivity. J. Clin. Invest. 2003; 112:902–914. [PubMed: 12975475]

17. Martinez X, Kreuwel HT, Redmond WL, Trenney R, Hunter K, Rosen H, Sarvetnick N, Wicker LS, Sherman LA. CD8+ T cell tolerance in nonobese diabetic mice is restored by insulin-dependent diabetes resistance alleles. J. Immunol. 2005; 175:1677–1685. [PubMed: 16034108]

18. Hultgren B, Huang X, Dybdal N, Stewart TA. Genetic absence of gamma-interferon delays but does not prevent diabetes in NOD mice. Diabetes. 1996; 45:812–817. [PubMed: 8635658]

19. Esensten JH, Lee MR, Glimcher LH, Bluestone JA. T-betdeficient NOD mice are protected from diabetes due to defects in both T cell and innate immune system function. J. Immunol. 2009; 183:75–82. [PubMed: 19535634]

20. Anderson MS, Bluestone JA. The NOD mouse: a model of immune dysregulation. Annu. Rev. Immunol. 2005; 23:447–485. [PubMed: 15771578]

21. Joseph J, Bittner S, Kaiser FM, Wiendl H, Kissler S. IL-17 silencing does not protect nonobese diabetic mice from autoimmune diabetes. J. Immunol. 2012; 188:216–221. [PubMed: 22116823]

22. Priyadharshini B, Welsh RM, Greiner DL, Gerstein RM, Brehm MA. Maturation-dependent licensing of naive T cells for rapid TNF production. PLoS ONE. 2010; 5:e15038. [PubMed: 21124839]

23. Martinez RJ, Zhang N, Thomas SR, Nandiwada SL, Jenkins MK, Binstadt BA, Mueller DL. Arthritogenic self-reactive CD4+ T cells acquire an FR4hiCD73hi anergic state in the presence of Foxp3+ regulatory T cells. J. Immunol. 2012; 188:170–181. [PubMed: 22124124]

24. Mohan JF, Levisetti MG, Calderon B, Herzog JW, Petzold SJ, Unanue ER. Unique autoreactive T cells recognize insulin peptides generated within the islets of Langerhans in autoimmune diabetes. Nat. Immunol. 2010; 11:350–354. [PubMed: 20190756]

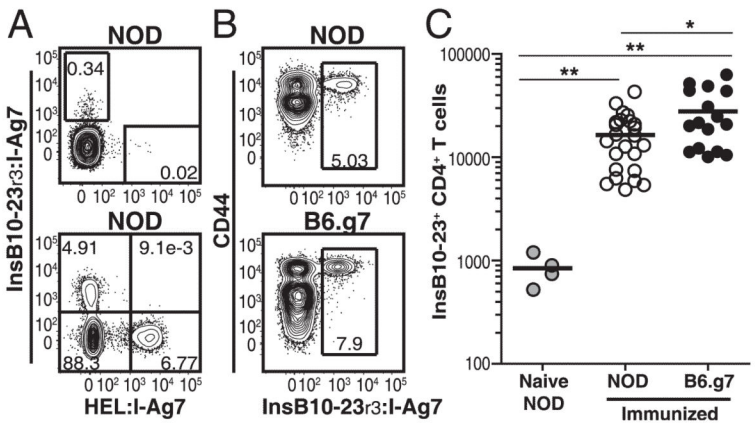

FIGURE 1.

Generation of the $InsB_{10–23r3}$:I-A^{g7} tetramer reagent. (**A**) $InsB_{10–23r3}$:I-A^{g7} and $HEL_{11–25}$:I-A^{g7} tetramer staining from spleen and nondLNs of naive (*top panel*) or immunized (*bottom panel*) nondiabetic NOD mice. (**B**) CD44 and $InsB_{10–23r3}$:I-A^{g7} from NOD or B6.g7 mice 8 d after immunization with $InsB_{10–23r3}$ or $HEL_{11–25}$ in CFA. (**C**) Enumeration of $InsB_{10–23r3}$-specific $CD4^+$ T cells in SLOs from NOD (n = 24) or B6.g7 (n = 17) mice postimmunization with $InsB_{10–23r3}$/CFA and control unimmunizedNOD mice (n = 4). Data in (B) and (C) are from five experiments. All flow cytometry was gated on singlet$^+$, $CD3^+$, $B220^–$, $CD11b^–$, $CD11c^–$, and $CD4^+$ cells. *p = 0.01–0.05, **p = 0.001–0.01.

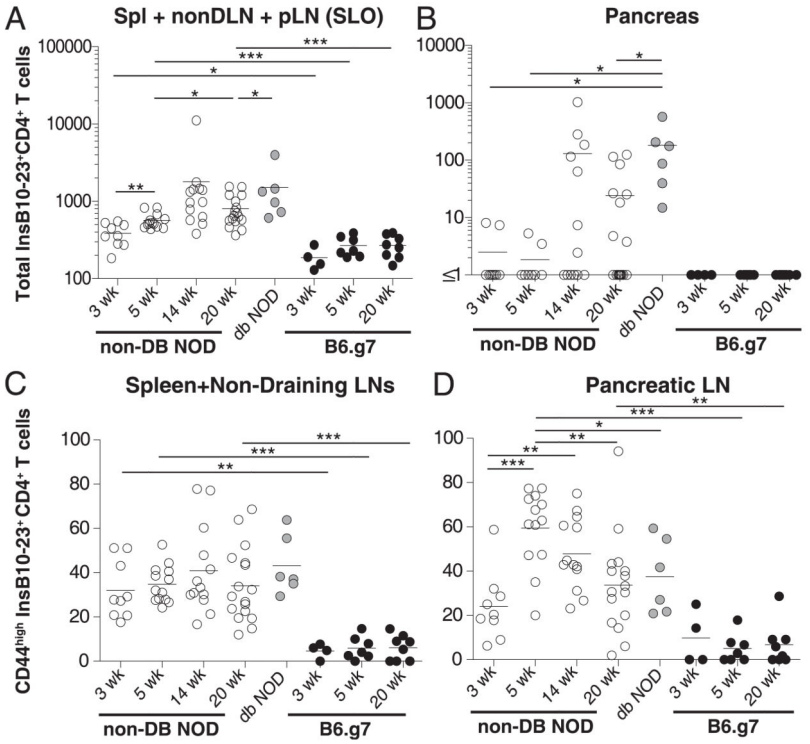

FIGURE 2.

Insulin-specific $CD4^+$ T cells only become activated and infiltrate the pancreas of NOD mice. Enumeration of $InsB_{10–23r3}$:I-A^{g7} cells in the pLNs, spleen,and non-dLNs combined (SLOs) (**A**) or pancreas (**B**) from NOD and B6.g7 mice. Frequency of $CD44^{high}$ insulin-specific $CD4^+$ T cells in the spleen and non-dLNs (**C**) and pLNs (**D**) from the NOD and B6.g7 mice shown in (A). Flow cytometry in (A) and (B) was gated on $singlet^+$, $CD3^+B220^-$, $CD11b^-$, $CD11c^-$, $CD4^+$, $CD8a^-$, $InsB_{10–23r3}$:I-A^{g7} PE^+, and $allophycocyanin^+$; flow cytometry in (C) and (D) also included CD44. Nondiabetic NOD at 3 wk (n = 9), 5 wk (n = 13), 14 wk (n = 13), and 20 wk (n = 17). Diabetic NOD mice (n = 6). B6.g7 mice at 3 wk (n = 4), 5 wk (n = 7), and 20 wk (n = 8). Data are compiled from 15 experiments. *p = 0.01–0.05, **p = 0.001–0.01, ***p < 0.001.

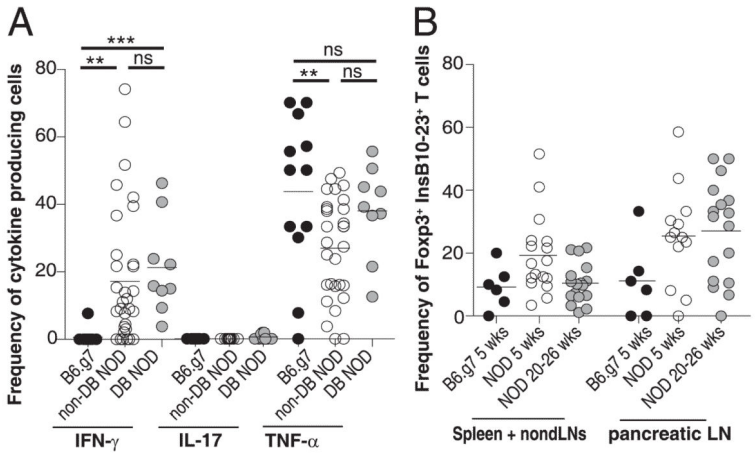

FIGURE 3.

Insulin-specific $CD4^+$ T cells produce the pathogenic cytokine IFN-γ in NOD mice but not B6.g7 mice. (**A**) Frequency of insulin-specific $CD4^+$ T cells from combined SLOs (Spl +nonDLN+pLN) producing IFN-γ, IL-17A, or TNF-α. Data are compiled from nine experiments with B6.g7 (n = 12), nondiabetic NOD (n = 28), and diabetic NOD (n = 9) mice. (**B**) Frequency of $Foxp3^+$ insulin-specific $CD4^+$ T cells in B6.g7 mice at 5 wk (n = 6), NOD mice at 5 wk (n = 17), and NOD mice at 20–26 wk (n = 17). Data are compiled from six experiments. Cells were gated on $singlet^+$, $B220^-$, $CD11b^-$, $CD11c^-$, $CD4^+$, $CD8a^-$, $InsB_{10–23r3}$:$I\text{-}A^{g7}$-PE^+ , and $InsB_{10–23r3}$:$I\text{-}A^{g7}$-$allophycocyanin^+$. $^{**}p$ = 0.001–0.01, $^{***}p$ < 0.001. ns, Not significant.

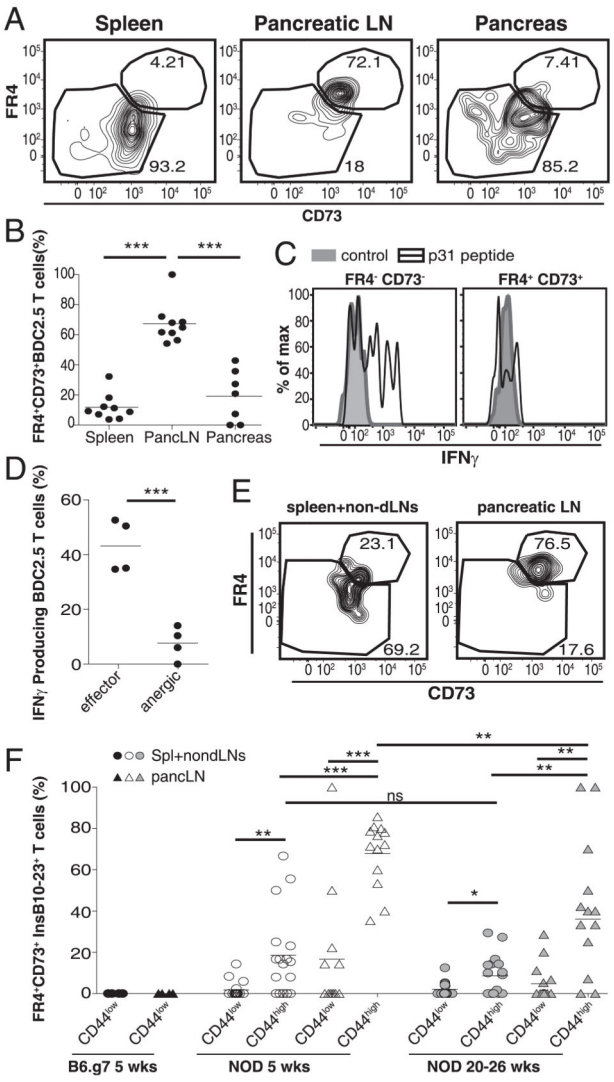

FIGURE 4.

Anergy is induced in islet-reactive CD4$^+$ T cells in NOD mice but not B6.g7 mice. (**A**) FR4 and CD73 expression on BDC2.5 T cells 17 d posttransfer. (**B**) Quantification of anergic BDC2.5 T cells in the spleen, pLNs, and pancreas 17–26 d posttransfer to nondiabetic NOD mice from three experiments. (**C**) IFN-γ production by effector (FR4$^-$CD73$^-$) and anergic (FR4$^+$CD73$^+$) phenotype BDC2.5 T cells in the pLNs at 56 d posttransfer. (**D**) Frequency of IFNg$^+$ BDC2.5 T cells in the pLNs at 56 d posttransfer. Data in (C) and (D) are representative from three experiments (n = 3–4). (**E**) FR4 and CD73 on insulin-specific CD4$^+$ T cells from a 5-wkold nondiabetic NOD mouse. (**F**) Frequency of anergic phenotype (Foxp3$^-$FR4$^+$CD73$^+$) insulin-specific CD4$^+$ T cells in the spleen+non-dLNs (circles) and the pLNs (triangles) from 5-wk-old B6.g7 mice (black, n = 6), 5-wk-old nondiabetic NOD mice (white, n = 17), and 20–26-wk-old nondiabetic NOD mice (gray, n = 17). Insulin-specific CD4$^+$ T cells were further gated on CD44^{high} versus CD44^{low} cells. Data are compiled from six experiments. Cells are gated on singlet$^+$, CD3$^+$, B220$^-$, CD11b$^-$, CD11c$^-$, CD4$^+$, Foxp3$^-$ cells. Data in (A)–(D) also include Thy1.1$^+$, CD44^{high} cells, and

data in (E) and (F) also include $InsB_{10–23r3}$:I-A^{g7} PE^{+} and allophycocyanin^{+} tetramers. *p = 0.01–0.05, **p = 0.001–0.01, ***p < 0.001. ns, Not significant.